



## Bioinformatics reveals diagnostic potential of cuproptosis-related genes in the pathogenesis of sepsis

Zhongyi Sun<sup>a,b,1</sup>, Qiuyue Zhao<sup>a,b,1</sup>, Jiahao Zhang<sup>a,b,1</sup>, Yanan Hu<sup>a,b</sup>, Jiachen Qu<sup>a,b</sup>, Han Gao<sup>c,\*\*</sup>, Zhiyong Peng<sup>a,b,\*</sup>

<sup>a</sup> Department of Critical Care Medicine, Zhongnan Hospital of Wuhan University, Wuhan, Hubei Province, 430071, China

<sup>b</sup> Clinical Research Center of Hubei Critical Care Medicine, Wuhan, Hubei, China

<sup>c</sup> Department of Respiratory and Critical Care Medicine, Zhongnan Hospital of Wuhan University, Wuhan, Hubei Province, 430071, China

### ARTICLE INFO

#### Keywords:

Sepsis  
ssGSEA  
GEO  
Immune  
Cuproptosis

### ABSTRACT

**Background:** Multiple modes of cell death occur during the development of sepsis. Among these patterns, cuproptosis has recently been identified as a regulated form of cell death. However, its impact on the onset and progression of sepsis remains unclear.

**Method:** We screened a dataset of gene expression profiles from patients with sepsis using the GEO database. Survival analysis was performed to analyze the relationship between cuproptosis-related genes (CRGs) and prognosis. Hub genes were identified through univariate Cox regression analysis. The diagnostic value of hub genes in sepsis was tested in both training sets (GSE65682) and validation sets (GSE134347). To examine the association between hub genes and immune cells, single-sample gene set enrichment analysis (ssGSEA) and Pearson correlation analysis were employed. Additionally, the CRGs were validated in a septic mouse model using real-time quantitative PCR (qRT-PCR) and immunohistochemistry (IHC).

**Results:** In sepsis, most CRGs were upregulated, with only DLD and MTF1 downregulated. High expression of three genes (GLE, LIAS, and PDHB) was associated with better prognosis, but only two hub genes (LIAS, PDHB) reached statistical significance. The receiver operating characteristic (ROC) analysis for diagnosing sepsis showed LIAS had a range of 0.793–0.906, while PDHB achieved values of 0.882 and 0.975 in the training and validation sets, respectively. ssGSEA analysis revealed a lower number of immune cells in the sepsis group, and there was a correlation between immune cell population and CRGs (LIAS, PDHB). Analysis in the septic mouse model demonstrated no significant difference in mRNA expression levels and IHC staining between LIAS and PDHB in heart and liver tissues, but up-regulation was observed in lung tissues. Furthermore, the mRNA expression levels and IHC staining of LIAS and PDHB were down-regulated in renal tissues.

**Conclusions:** Cuproptosis is emerging as a significant factor in the development of sepsis. LIAS and PDHB, identified as potential diagnostic biomarkers for cuproptosis-associated sepsis, are believed to play crucial roles in the initiation and progression of cuproptosis-induced sepsis.

\* Corresponding author. Department of Critical Care Medicine, Zhongnan Hospital of Wuhan University, Wuhan, Hubei Province, 430071, China.

\*\* Corresponding author.

E-mail addresses: [2022103030001@whu.edu.cn](mailto:2022103030001@whu.edu.cn) (H. Gao), [pengzy5@whu.edu.cn](mailto:pengzy5@whu.edu.cn) (Z. Peng).

<sup>1</sup> Zhongyi Sun, Qiuyue Zhao, and Jiahao Zhang contributed equally to this work and shared the first authorship.

## 1. Introduction

Sepsis is a life-threatening condition characterized by organ dysfunction resulting from an unregulated host response to infection [1]. Despite efforts to prevent underlying conditions such as hypertension [2], substantial investments in healthcare and infrastructure [3], as well as patient mental health [4], sepsis continues to be a significant global health concern with high incidence and mortality rates. The pathogenesis of sepsis involves various mechanisms, including pathogen invasion, cytokine release, microcirculation dysfunction, immune imbalances and cell death [5]. The predetermined [6], precisely controlled programmed cell death modes [7] that have been reported include apoptosis [8], pyroptosis [9], autophagy [10], necrosis [8], and ferroptosis [11]. The complex pathophysiology necessitates the identification of reliable diagnostic markers and therapeutic targets to improve patient outcomes.

Cuproptosis, a newly discovered form of regulated cell death, has emerged as a potential contributor to sepsis pathology. Cuproptosis involves dysregulation of copper homeostasis [12], where copper directly binds to lipid components of the tricarboxylic acid (TCA) cycle, leading to cellular oxidative stress and subsequent cell death [13]. Several studies have demonstrated the close association between cuproptosis and development of various cancers [12], including clear cell renal cell carcinoma [14] and hepatocellular carcinoma [15]. Understanding the molecular mechanisms underlying cuproptosis and its relationship with sepsis could facilitate the discovery of novel biomarkers and therapeutic interventions.

In sepsis, disturbances in ionic equilibrium, particularly involving iron and copper, can disrupt mitochondrial function [16]. Ferroptosis is regulated by factors such as iron-dependent phospholipid peroxidation, reduced glutathione levels, and the GPX4 inactivation, plays a role in this process [17]. Elevated intracellular iron levels during sepsis promote bacterial overgrowth, while infection-induced fatty acids and ROS trigger lipid peroxidation, activating ferroptosis and potentially contributing to multiple organ failure [18].

Similarly, systemic or local acidosis in the initial phase of sepsis can lead to the release of copper from ceruloplasmin and other proteins [19], resulting in increased circulating copper ions. Free copper can oxidize catecholamines *in vitro*, leading to their inactivation and potentially contributing to the pathogenesis of sepsis [20]. The modulation of copper levels has been demonstrated to effectively counteract the anticoagulant effects of activated protein C in the treatment of sepsis [21]. The presence of excessive copper ions can induce a specific type of cell death referred to as cuproptosis. However, the detailed understanding of the relationship between cuproptosis and sepsis remains incomplete, as only a limited number of studies have investigated the potential correlation between sepsis and cuproptosis by examining the role of cuproptosis-associated genes (CRGs) in early sepsis diagnosis. In this study, the aim of this study was to utilize bioinformatics approaches to identify CRGs that may serve as diagnostic markers for sepsis.

Overall, this study provided novel insights on sepsis and cuproptosis, exploring the potential diagnostic values of CRGs. The findings may have the potential to facilitate the development of novel diagnostic tools and targeted therapies for sepsis, ultimately improving patient outcomes and alleviating the burden of this devastating condition.

## 2. Materials and methods

### 2.1. Analysis of the roles of CRGs in sepsis from the gene datasets

#### 2.1.1. Gene expression profile data preparation

The gene expression profile dataset of sepsis patients was obtained from the Gene Expression Omnibus (GEO) database [22]. The GSE65682 dataset, based on GPL3667 (Affymetrix Human Genome U219 Array), contained 760 sepsis and 42 healthy subjects. GSE134347 was based on a GPL17586 dataset of 156 sepsis patients, 83 healthy subjects, and 59 uninfected critically ill patients. GSE65682 and GSE134347 were used as the training set and validation set for additional analysis, respectively.

#### 2.1.2. Acquisition, difference analysis, and expression correlation analysis of CRGs

The CRGs were obtained from an original scientific research paper, including DLD, PDHA1, DLAT, LIPT1, FDX1, PDHB, MTF1, CDKN2A, LIAS, and GLS [23]. The “Limma” package was used to analyze differences in CRG expression between sepsis and healthy subjects. Genes with  $\log_2(|\text{FoldChange}|) > 1$  and  $\text{adjust } P < 0.05$  were considered as screening criteria for Differentially Expressed Genes (DEGs). The “pheatmap” package was used to draw a differential expression heatmap, and the “corrplot” package was used for correlation analysis between CRGs and to create an association analysis chart.

#### 2.1.3. Construction of protein-protein interaction networks

The String database, which searches for known and predicted interactions between proteins, was used to construct the CRG protein-protein interaction network. The network was visualized using Cytoscape 3.9.1 (<https://cytoscape.org/>) [24]. The key genes were screened by CytoHubba plug in Cytoscape [25].

#### 2.1.4. Identification and validation of hub genes

Kaplan-Meier survival analysis was used to assess the relationship between CRGs and patient survival. A significance level of  $P < 0.05$  was considered statistically significant. Univariate Cox analysis was conducted to identify characteristics significantly associated with survival. The “pROC” package in R was used for ROC analysis, and the Area Under Curve (AUC) value was calculated to evaluate the diagnostic efficacy of CRG genes associated with survival in sepsis patients. An AUC index  $> 0.85$  was considered to indicate good diagnostic performance. Hub genes were validated using the GSE134347 dataset.

### 2.1.5. Clinical relevance of hub genes

To identify the effect of different clinical traits on the expression of hub genes, the clinical information of patients published in the GSE65682 dataset, including gender and age, was obtained. The patients were classified into two groups:  $\geq 65$  years old and  $< 65$  years old. Pearson correlation analysis was used to identify correlations between hub gene expression and age and gender.

### 2.1.6. Nomogram construction

A diagnostic risk score was constructed based on the expression levels of hub genes in sepsis. Sepsis rates were predicted based on clinical factors and genes, which were used to construct the Nomogram for diagnosis [26].

### 2.1.7. Immune infiltration analysis

Single-sample gene set enrichment analysis (ssGSEA) was used as the immune infiltration algorithm to analyze the content of 24 immune cells in each sample in the GSE65682 dataset [27]. The Wilcoxon rank sum test was used to compare the difference in immune cells between sepsis and healthy subjects. Spearman correlation was used to analyze the relationship between hub CRGs and immune cell infiltration.  $P < 0.05$  was considered statistically significant.

### 2.1.8. Gene set enrichment analysis (GSEA)

GSEA was performed to further explore the role of hub CRGs in sepsis [28]. GSEA uncovered the potential mechanisms of hub genes through the Molecular Signatures Database (MSigDB, <http://software.broadinstitute.org/gsea/msigdb/index.jsp>), specifically the c2 (c2.kegg.v2022.1.Hs.symbols.gmt) and c5 (c5.all.v2022.1.Hs.symbol.gmt) [29]. Results with a false discovery rate (FDR)  $< 0.25$  and a nominal  $P$ -value  $< 0.05$  were considered statistically significant.

## 2.2. Mice experiments to validate the findings

The animal experiment was approved by Wuhan University. The sepsis model was established using cecal ligation and puncture (CLP) in male C57BL/6 mice (8–12 weeks old). The mice were anesthetized by intraperitoneal injection of pentobarbital sodium (1 %, Sigma, USA) at a dose of 50 mg/kg. A midline incision of approximately 1 cm was made in the lower abdomen. In the CLP group, the cecum was dissected and ligated, and then punctured twice with a 20 g puncture needle. The cecum was gently squeezed to push the excrement into the abdominal cavity, and then the cecum was anastomosed and the abdomen closed. Volumetric resuscitation was promptly performed using ringer saline (25 ml/kg). In contrast, the mice in the sham group underwent the same procedure, but without the additional treatment mentioned for the CLP group. After 24 h, serum, heart, liver, lungs, and kidneys were collected from both groups of mice for subsequent detection and experiments.

### 2.2.1. Quantitative real-time polymerase chain reaction (qRT-PCR) analysis

Total RNA was extracted from the heart, liver, lungs, and kidneys of CLP and sham mice using the FastPure Plant Total RNA Isolation Kit (Vazyme, Nanjing, China). Besides, cDNA was synthesized using the ReverTra Ace Kit (Toyobo, Osaka, Japan). The qRT-PCR was performed on the LightCycler 96 Real-Time PCR Detection System (Hoffmann-La Roche Ltd., Shanghai, China) using SYBR Green PCR mix.

### 2.2.2. Histology and immunohistochemistry (IHC) analyses

The heart, liver, lungs, and kidneys of mice in the CLP and sham groups were fixed in 10 % formaldehyde and then dehydrated in 70 % ethanol. Tissue sections (5  $\mu\text{m}$ ) were prepared and embedded in paraffin. The sections were dehydrated using graded alcohol, and the antigens were retrieved using heated citrate buffer. Antibodies against LIAS (11577-1-AP, ProteinTech, Wuhan, China) and PDHB (14744-1-AP, ProteinTech, Wuhan, China) were purchased from ProteinTech (Wuhan, China). Five random fields were examined under light microscopy (Nikon, Japan).

### 2.2.3. Enzyme-linked immunosorbent assay (ELISA)

Cardiac blood samples were collected from mice in both groups in sterile 1.5 ml centrifuge tubes and centrifuged at 3000 rpm for 15 min after the serum had naturally precipitated. Serum creatinine (S03036) and urea nitrogen (S03076) levels were measured using ELISA according to the manufacturer's instructions.

## 2.3. Statistical analysis

All statistical analyses were conducted using R software (version 4.2.0) and GraphPad Prism (version 9.0), and corresponding visualizations were generated. Two independent-sample  $t$ -tests or Mann-Whitney  $U$  tests were used to determine significant differences between groups. Pearson correlation analysis was used to evaluate the correlation among the expression of CRGs and the correlation between hub genes and clinical traits. Kaplan-Meier survival analysis was utilized to evaluate the relationship between CRG expression and patient survival. Univariate Cox analysis was performed to identify characteristics significantly associated with survival. The significance level was set at  $P < 0.05$ .

### 3. Results

#### 3.1. Identification of cuproptosis-related DEGs in sepsis

The GSE65682 and GSE134347 datasets were downloaded from the GEO database, and DEGs between sepsis and normal samples were screened based on the criteria of  $|\log FC| \geq 1$  and  $P < 0.05$ . Fig. 1A shows the standardized expression of cuproptosis-related DEGs in a heatmap. Ten genes were identified to be significantly associated with cuproptosis, with two up-regulated and eight down-regulated. Furthermore, correlation analysis revealed a positive correlation between the expression of PDHB and LIAS, LIPT1, FDX1, and DLAT. Additionally, LIAS showed a positive correlation with LIPT1 and FDX1 (Fig. 1B).

#### 3.2. Establishment of PPI network and identification of key genes

The STRING database was used to construct the PPI network to assess the interactions between proteins corresponding to the DEGs. The network was visualized using Cytoscape software, consisting of 10 nodes and 23 edges. Two proteins did not have any connections with other proteins and did not form a protein network (Fig. 1C). The intensity of the protein color indicates the strength of the evidence for protein-protein interactions. The analysis identified LIAS, PDHA1, and DLD as the three strongest genes in the network. The CytoHubba plugin in Cytoscape confirmed that LIAS, PDHA1, and DLD were the key genes in the PPI network (Fig. 1D).

#### 3.3. Survival analysis

To evaluate the prognostic value of the candidate genes, 479 sepsis patients in the GSE65682 dataset were divided into high- and low-expression groups based on their DEG levels. High expression levels of LIAS ( $P = 0.007$ ), GLS ( $P = 0.029$ ), and PDHB ( $P < 0.001$ ) were associated with a favorable prognosis (Fig. 2A, B, and C). However, the other genes did not influence the prognosis of sepsis (Fig. 2D, E, F, G, H, I, and J). In summary, LIAS, GLS, and PDHB have the potential to be prognostic biomarkers for sepsis.

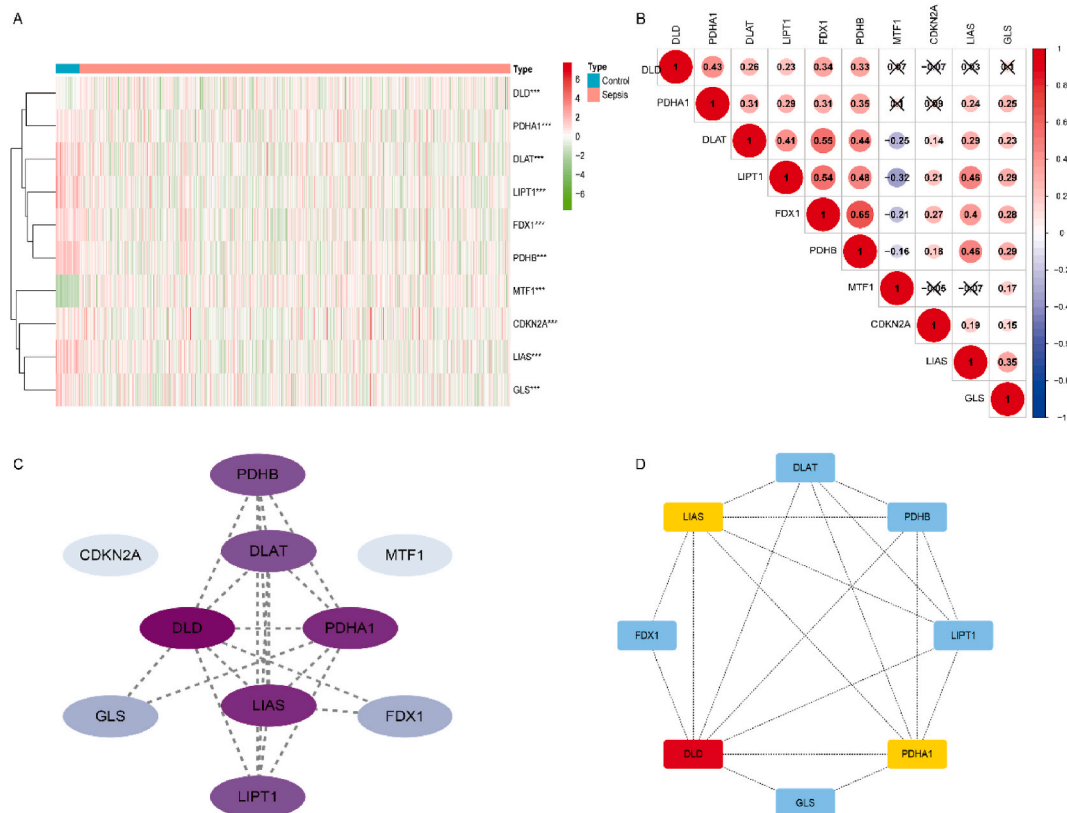


**Fig. 1.** (A) Heatmap of cuproptosis-related genes (CRGs) in GSE65682 database. (B) Expression correlation analysis of CRGs. (C) Protein-protein interaction (PPI) networks of CRGs. (D) Determination of key genes from the PPI network.



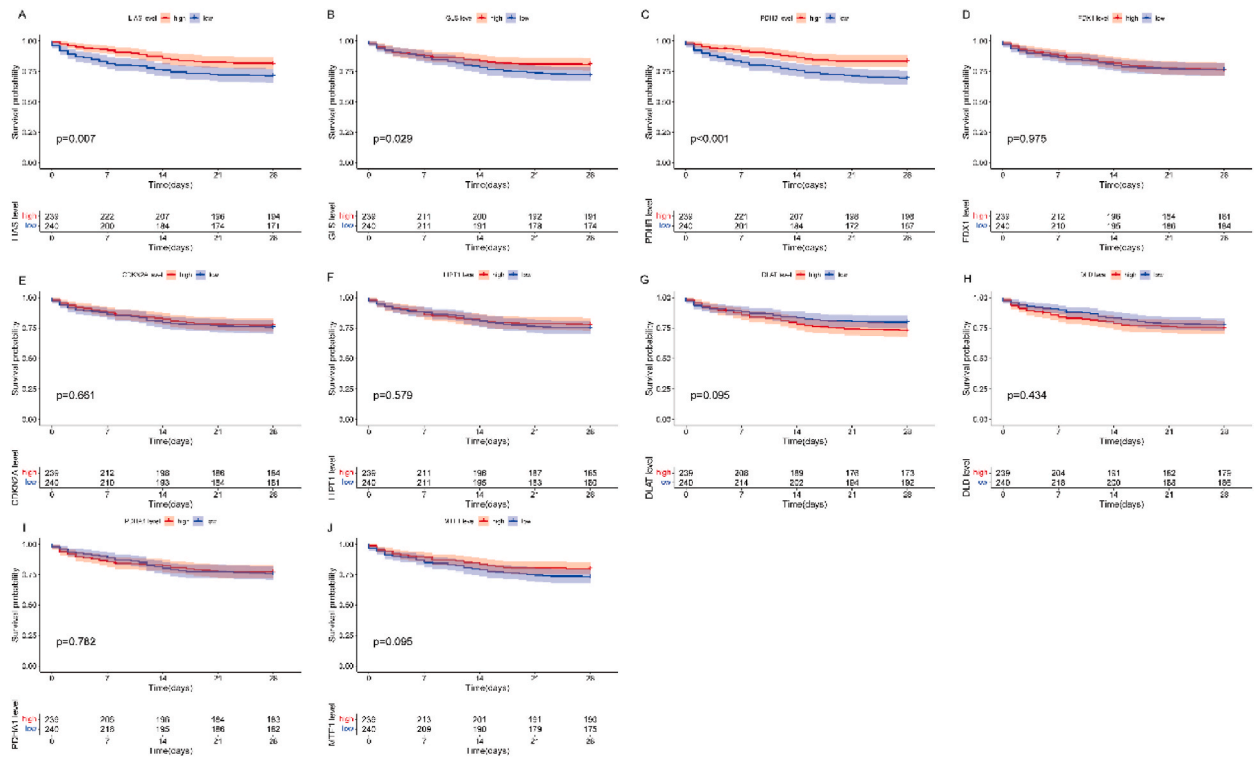


**Fig. 2.** Kaplan–Meier plot for the expression of (A) LIAS; (B) GLS; (C) PDHB; (D) FDX1; (E) CDKN2A; (F) LIPT1; (G) DLAT; (H) DLD; (I) PDHA1; (J) MTF1.

**3.4. Prognosis-related analysis**

Univariate Cox regression analysis was used to estimate the hazard ratio (HR) of survival. LIAS and PDHB were significantly negatively associated with survival ( $P < 0.05$ ) (Fig. 3A). In addition, the time-dependent receiver operating characteristic (ROC) curve analysis showed AUC values of 0.351, 0.390, and 0.410 for LIAS at 1, 2, and 3 weeks, respectively (Fig. 3B). For PDHB, the AUC values were 0.409, 0.411, and 0.402 at 1, 2, and 3 weeks, respectively (Fig. 3C).

**3.5. Differential expression analysis and ROC analysis**

The two candidate CRGs were analyzed through training and validation. Differential expression analysis revealed significantly lower expression levels of LIAS and PDHB in the sepsis group compared to the control group in both the training and test datasets (Fig. 4A, B, E, F). The AUC values for LIAS and PDHB were 0.860 and 0.954 in the training set (Fig. 4C and D), respectively, and 0.839 and 0.913 in the test set (Fig. 4G and H).

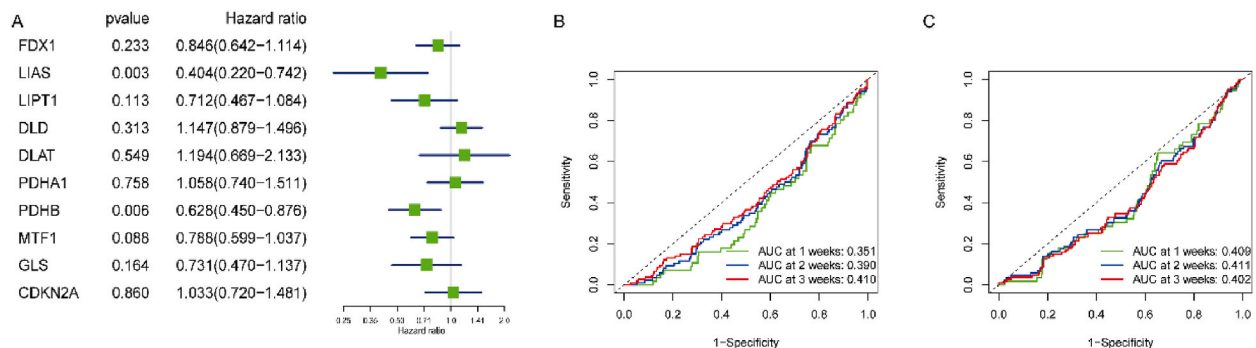


**Fig. 3.** (A) Hazard ratios and p-value of the constituents involved in univariate Cox analysis. ROCs for one-week, two-week and three-week survival prediction of (B) LIAS; (C) PDHB.

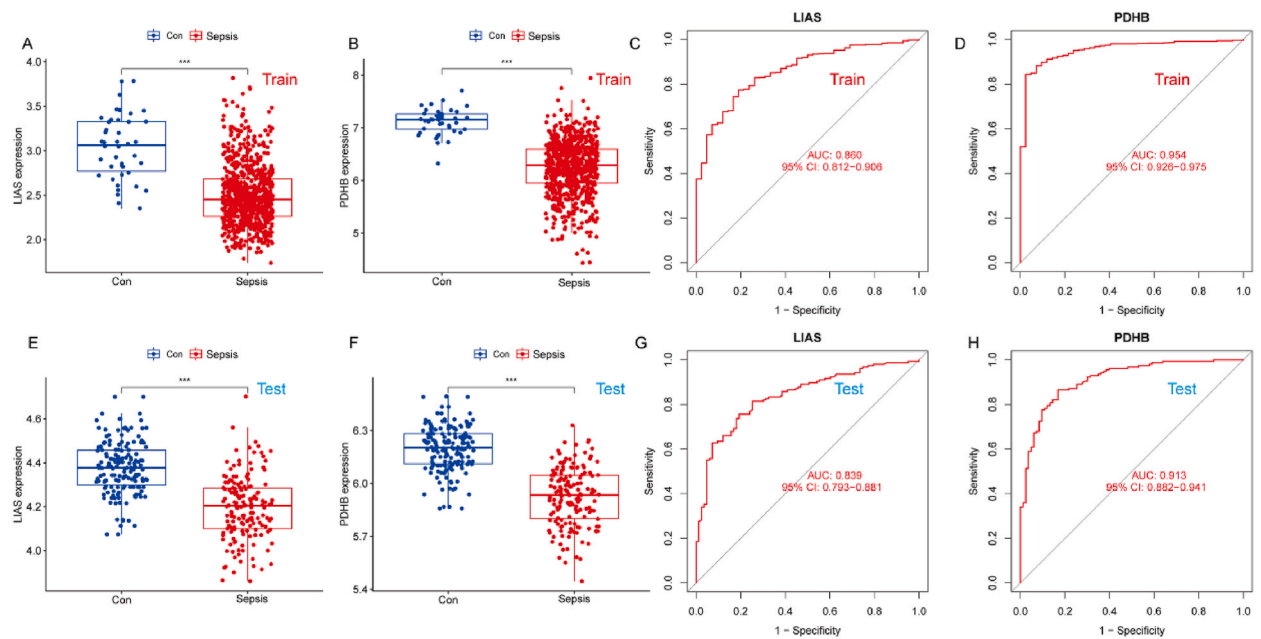


**Fig. 4.** The performance of hub genes to diagnose sepsis in GSE65682 (A) Expression difference of LIAS in the sepsis and control groups; (B) Expression difference of PDHB in the sepsis and control groups. (C) ROC curve of LIAS; (D) ROC curve of PDHB. The performance of hub genes to diagnose sepsis in the GSE13904 validation sets; (E) Expression difference of LIAS gene in the sepsis and control groups; (F) Expression difference of PDHB gene in the sepsis and control groups; (G) ROC curve of LIAS. (H) ROC curve of PDHB.

### 3.6. Hierarchical analysis of differential expression and nomogram construction

Sepsis patients were categorized by gender and age, and the expression of LIAS and PDHB was analyzed and compared. As shown in the boxplots in Fig. 5A–D, the expression level of PDHB was upregulated in the age <65 group ( $P = 0.04$ ). There were no statistically significant differences in LIAS expression among different age groups ( $P = 0.1$ ), and there were no significant differences in the expression levels of LIAS ( $P = 0.81$ ) and PDHB ( $P = 0.82$ ) between gender groups. To predict the possibility of sepsis, a nomogram model was constructed for risk assessment of prognostic patients based on the gene expression levels of LIAS and PDHB as a function of age and sex (Fig. 5E). The overall calibration showed that both the apparent calibration curve and the bias-corrected curve were within an appropriate range and did not deviate too far from the ideal curve (Fig. 5F).

### 3.7. Immune cell enrichment analysis

The ssGSEA was performed to explore the relationship between these two genes and multiple immune cell populations. The sepsis group showed enrichment in activated dendritic cells, type 17 T helper cells, gamma delta T cells, regulatory T cells, monocytes, neutrophil mast cells, and plasmacytoid dendritic cells. Additionally, effector memory CD8 T cells, central memory CD8 T cells, activated CD8 T cells, effector memory CD4 T cells, central memory CD4 T cells, activated CD4 T cells, CD56dim natural killer cells, immature B cells, activated B cells, memory B cells, type 1 helper cells, natural killer T cells, MSDC T follicular helper cells, CD56bright natural killer cells, monocytes, and immature dendritic cells compared to the sepsis group (all  $P$  values < 0.05) (Fig. 6A–B). Furthermore, LIAS showed a significant positive correlation with the abundance of type 2 T helper cells, type 1 T helper cells, natural killer T cells, monocytes, memory B cells, myeloid-derived suppressor cells (MDSCs), macrophages, immature dendritic cells, immature B cells, effector memory CD8 T cells, effector memory CD4 T cells, central memory CD8 T cells, central memory CD4 T cells, activated CD8 T cells, activated CD4 T cells, and activated B cells. It showed a negative correlation with type 17 T helper cells, natural killer cells, macrophages, CD56dim natural killer cells, and activated dendritic cells. On the other hand, PDHB was negatively correlated with type 17 T helper cells, neutrophils, natural killer cells, eosinophils, CD56dim natural killer cells, and activated dendritic cells. It was positively associated with type 1 T helper cells, T follicular helper cells, regulatory T cells, plasmacytoid dendritic cells, natural killer T cells, monocytes, memory B cells, MDSCs, immature dendritic cells, immature B cells, gamma delta T cells, effector memory CD8 T cells, effector memory CD4 T cells, central memory CD4 T cells, CD56bright natural killer cells, activated CD8 T cells, activated CD4 T cells, and activated B cells (all  $P$  values < 0.05) (Fig. 6C).

### 3.8. GSEA

Gene functional enrichment analysis was performed using GSEA. The GO enrichment terms showed that LIAS was mainly

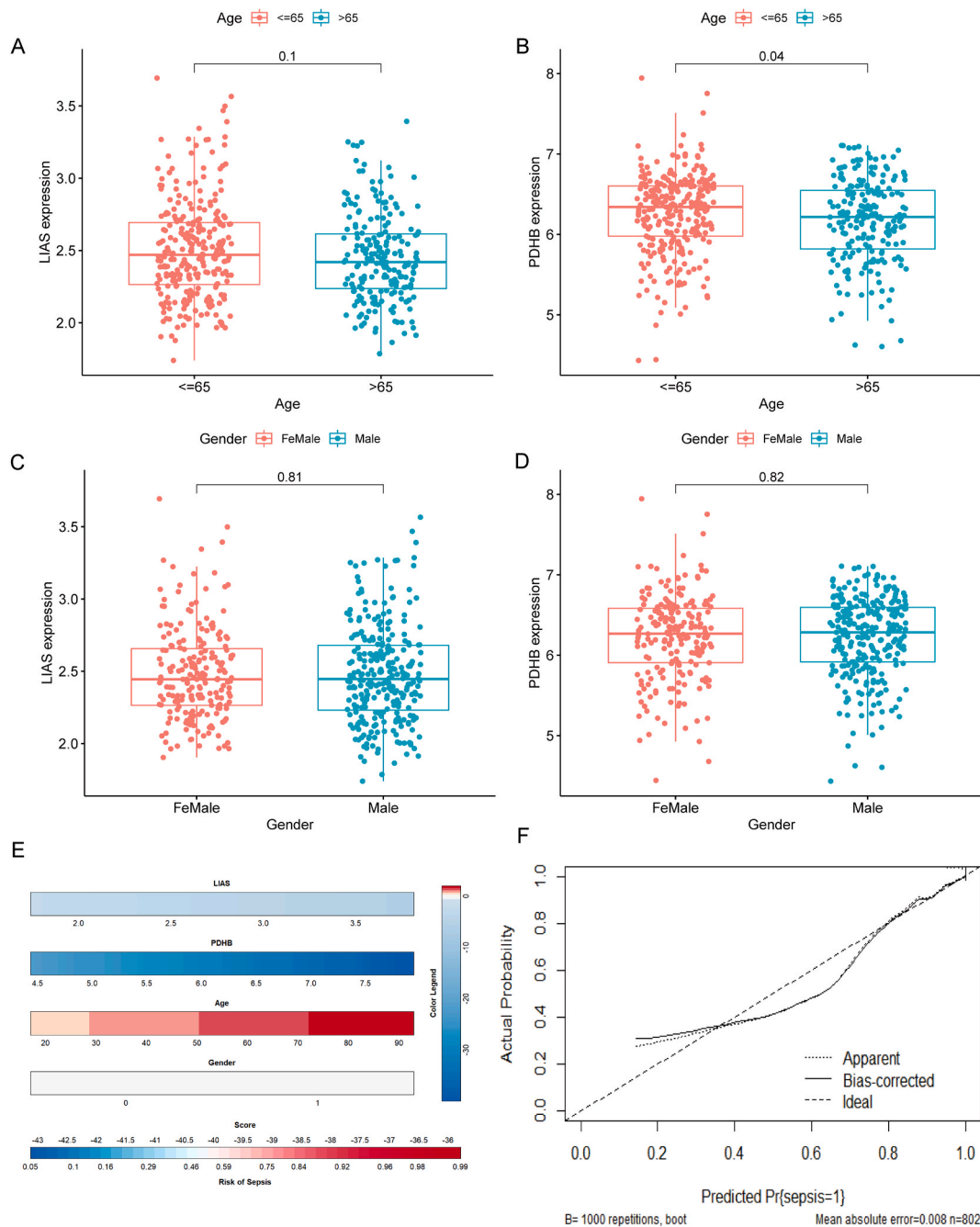


**Fig. 5.** (A) Expression of LIAS in sepsis and normal controls grouped by age; (B) Expression of PDHB in sepsis and normal controls grouped by age; (C) Expression of LIAS in sepsis and normal controls grouped by gender; (D) Expression of PDHB in sepsis and normal controls grouped by gender. (E) Nomogram combined the two hub genes (LIAS and PDHB); (F) Calibration plots of probabilities; gender (0 = Female, 1 = Male).

associated with growth factor activity, abnormal glomerular mesangium morphology, and diffuse mesangial sclerosis (Fig. 7A–C). Additionally, PDHB was mainly associated with the TCA cycle, the citrate cycle, and the intrinsic components of the mitochondrial inner membrane (Fig. 7D–F).

### 3.9. Validate the expression of hub genes in the mouse sepsis model

The serum levels of creatinine and urea nitrogen were found to be higher in septic mice compared to the control group, as determined by ELISA (Fig. 8A–B). As described earlier, qPCR and IHC analysis were performed on the septic mice. In the sepsis mouse

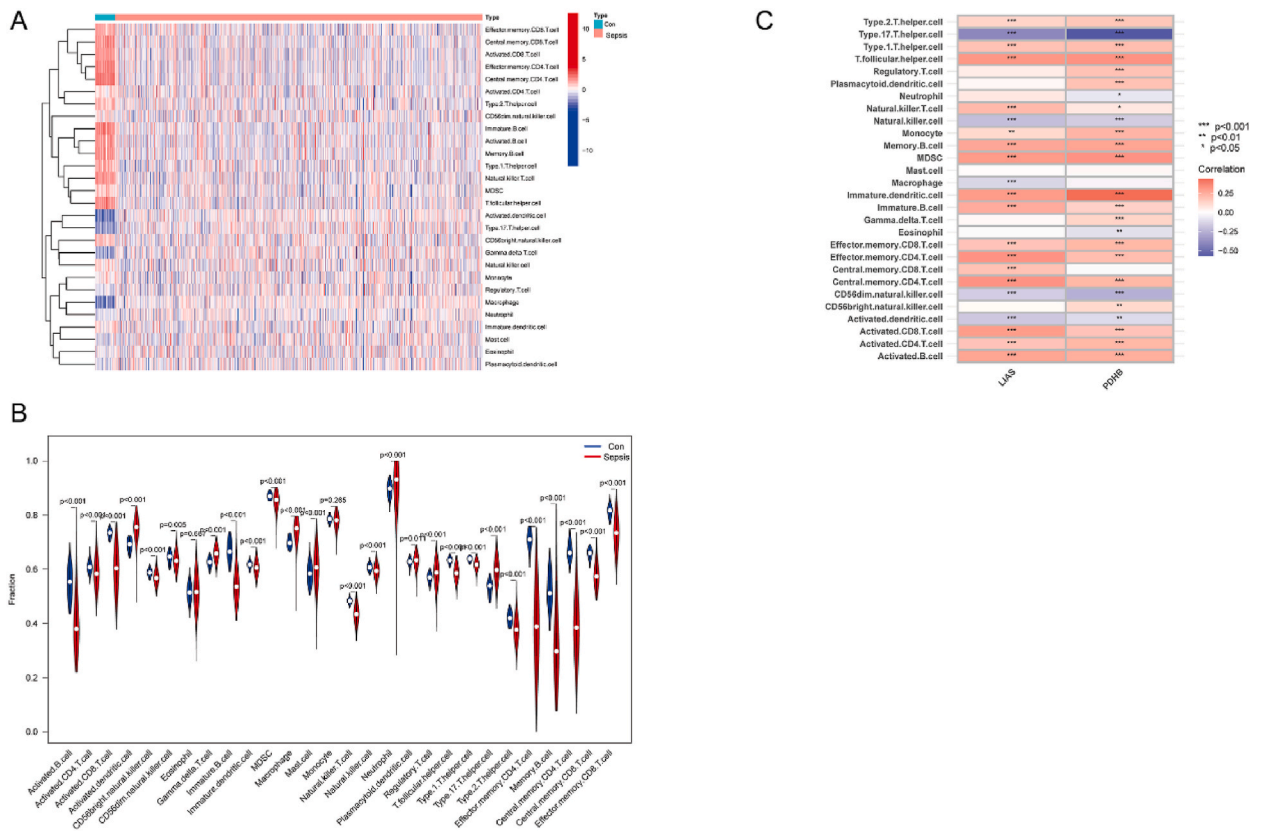


**Fig. 6.** (A) Heatmap of infiltrated immune cells in sepsis; (B) Expression levels of immune cells in sepsis and normal controls; (C) Immune cell correlation analysis of LIAS and PDHB.

model, a decrease in LIAS and PDHB mRNA expression was observed in the kidney, while an increase was observed in the lung (Fig. 8C–D). The expression of LIAS and PDHB in the tissues was also detected by IHC, and the same results were observed (Fig. 9A–H).

**4. Discussion and limitations**

This study investigated the DEGs associated with cuproptosis in sepsis. Sepsis, a severe infectious disease, often induces mitochondrial dysfunction and metabolic disturbances in patients, which disrupt cellular energy metabolism. Through PPI network analysis, three key genes—LIAS, PDHA1, and DLD—were identified in the relationship between sepsis and cuproptosis. These genes play crucial roles in energy metabolism and cellular function. LIAS [30] is involved in fatty acid synthesis, PDHA1 [31] converts pyruvate to acetyl-CoA, and DLD [32] participates in electron transfer reactions. In cuproptosis, the toxic effects of copper ions can interfere with LIAS and PDHA1, disrupt the structure and activity of DLD, and impact cellular energy generation and metabolism. Almost all of the CRGs were up-regulated in sepsis, except for DLD and MTF which were down-regulated. Elevated expressions of three genes (GLE, LIAS, PDHB) were associated with a favorable prognosis, but after the univariate COX regression analysis, only two hub genes (LIAS, PDHB) showed statistical significance. Furthermore, LIAS and PDHB were found to have accurate diagnostic values in the training set GSE65682 as measured by ROC (all AUC>0.85). The ROC analysis of LIAS and PDHB in diagnosing sepsis in the validation set GSE134347 was also remarkable (all AUC>0.8). Moreover, a negative correlation was observed between PDHB expression and age. The number of immune cells in the sepsis group decreased and was positively correlated with LIAS and PDHB. It is reasonable to speculate that CRGs may potentially affect sepsis by regulating the distribution of immune cells. However, the specific mechanism needs to be verified in future studies. In the sepsis mouse model, we observed decreased expression of LIAS and PDHB mRNA in the kidney and increased expression in the lung. IHC yielded consistent results. In summary, the expression of CRGs, LIAS and PDHB, was lower in sepsis. This suggests that LIAS and PDHB may act as negative regulators of sepsis and play an indispensable role in sepsis diagnosis.

Lipoic acid synthase (LIAS) is responsible for encoding the components of the lipoic acid pathway and synthesizing  $\alpha$ -Lipoic acid (LA), which is a potent antioxidant found in mitochondria [33]. Mutations in the LIAS gene can lead to impaired enzyme activity and disruption of the normal process of long-chain fatty acid oxidation, leading to an accumulation of fatty acid intermediates. This abnormality can trigger oxidative stress through lipid peroxidation and the production of reactive oxygen species (ROS) [34]. Moreover, it has been established that oxidative stress itself can modulate the expression and function of the LIAS gene. Multiple studies have



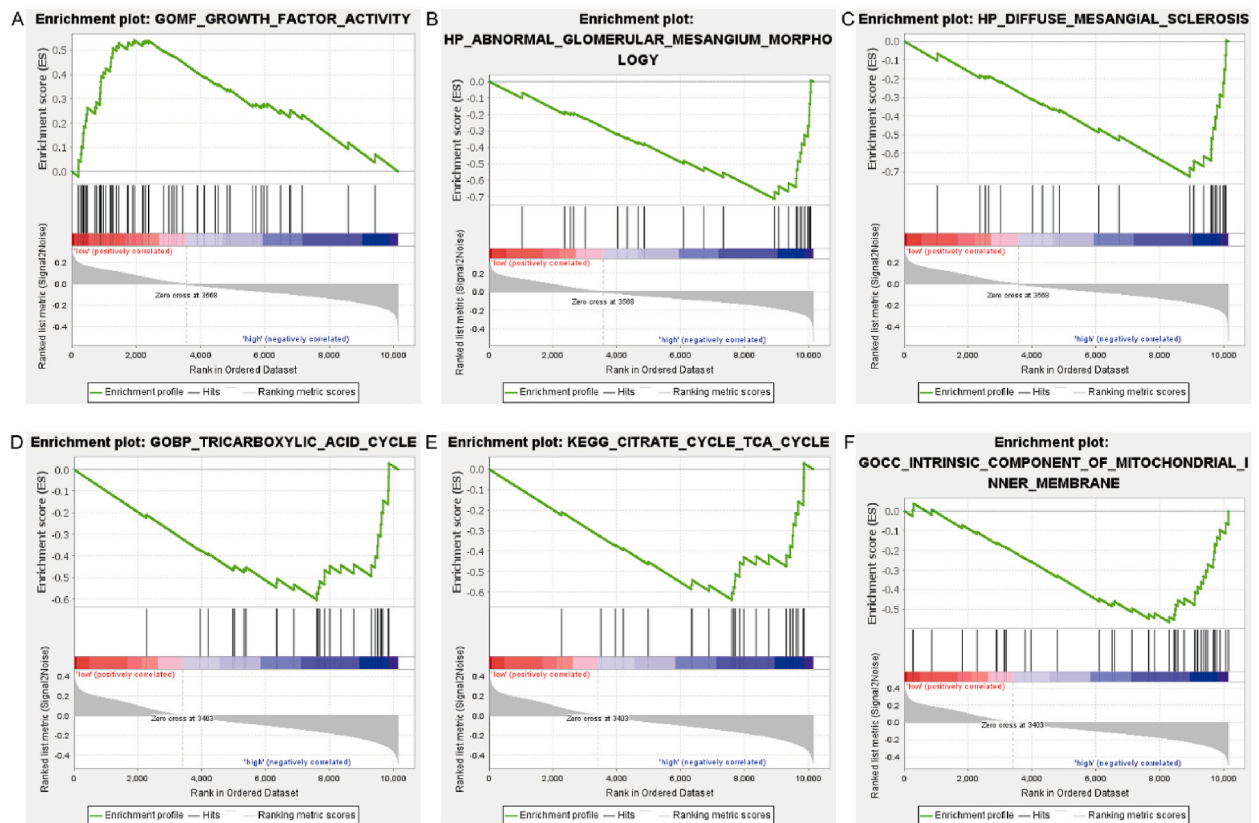


**Fig. 7.** GSEA analysis of LIAS: (A) Growth factor activity; (B) Abnormal glomerular mesangium morphology; (C) Diffuse mesangial sclerosis. GSEA analysis of PDHB: (D) Tricarboxylic acid (TCA) cycle; (E) Citrate cycle; (F) Intrinsic component of mitochondrial inner membrane.

demonstrated that oxidative stress influences gene expression by means of epigenetic modifications and signaling pathways involving transcription factors, thus exacerbating the metabolic dysfunction associated with LIAS-related diseases [35]. In this study, we also observed a decrease in LIAS expression during sepsis. Similar findings were reported by Kuikwon, who demonstrated reduced LIAS gene expression in mice induced with lipopolysaccharide (LPS). This decrease impairs the body's ability to resist oxidative stress and neutrophil recruitment, ultimately resulting in tissue damage [36]. Another study revealed that down-regulation of LIAS leads to reduced levels of endogenous long-chain fatty acid and impairing crucial mitochondrial antioxidant activities. As a consequence, an imbalance in REDOX status, subsequent inflammation, as well as mitochondrial dysfunction occur [37]. During the development of sepsis, the body's organs respond to increased oxidative stress by reducing the oxidative metabolism of glucose [38]. In conclusion, the decreased expression of LIAS genes in sepsis is closely associated with oxidative stress, mitochondrial dysfunction, and a decline in endogenous antioxidant reserves. This emphasizes the crucial role of LIAS in maintaining redox balance and proper mitochondrial function in the context of sepsis. In a recent study on diabetic nephropathy, it was discovered that decreased expression of LIAS resulted in excessive oxidative stress in the kidney, leading to energy deficiency and dysfunction in the proximal renal tubules [39]. In our current study, we observed a correlation between LIAS and glomerular mesangial abnormalities, which could potentially contribute to abnormal renal metabolic function in sepsis. Additionally, there seems to be a relationship between LIAS and neutrophils. Further investigation would be required to elucidate the specific molecular regulatory mechanisms involved.

PDHB, one of the crucial enzymes in the Krebs cycle, plays a pivotal role in cellular energy metabolism by converting acetyl-CoA and facilitating its entry into the TCA cycle, ultimately leading to ATP generation. This underscores the significant importance of PDHB in ensuring efficient cellular energy production (38). Mitochondrial dysfunction inhibits the TCA cycle, resulting in the accumulation of excessive reactive oxygen species (ROS), which impairs cellular energy metabolism (34). In our research, we also identified a noteworthy molecular pathway involving PDHB's interaction with the mitochondrial inner membrane. Through gene set enrichment analysis (GSE), we discovered intrinsic components of the mitochondrial inner membrane that could potentially be regulated by PDHB expression, indicating its involvement in mitochondrial function regulation. Within the mammalian retina, the (pro)renin receptor ATP6/AP2 binds to the E1 subunit of PDHB and, by affecting PDHB phosphorylation, regulates aerobic glucose metabolism and oxidative stress (39). In the context of sepsis, dysregulation of carbohydrate, amino acid, and glucose metabolism occurs due to an excessive inflammatory response, leading to ROS overproduction and subsequent cell and tissue damage (40). Some researchers have found a potential correlation between obesity (41) and improved prognosis in septic patients. Obesity may confer certain benefits in sepsis by providing a protective energy reserve, preventing muscle loss in the highly catabolic state, and regulating the immune

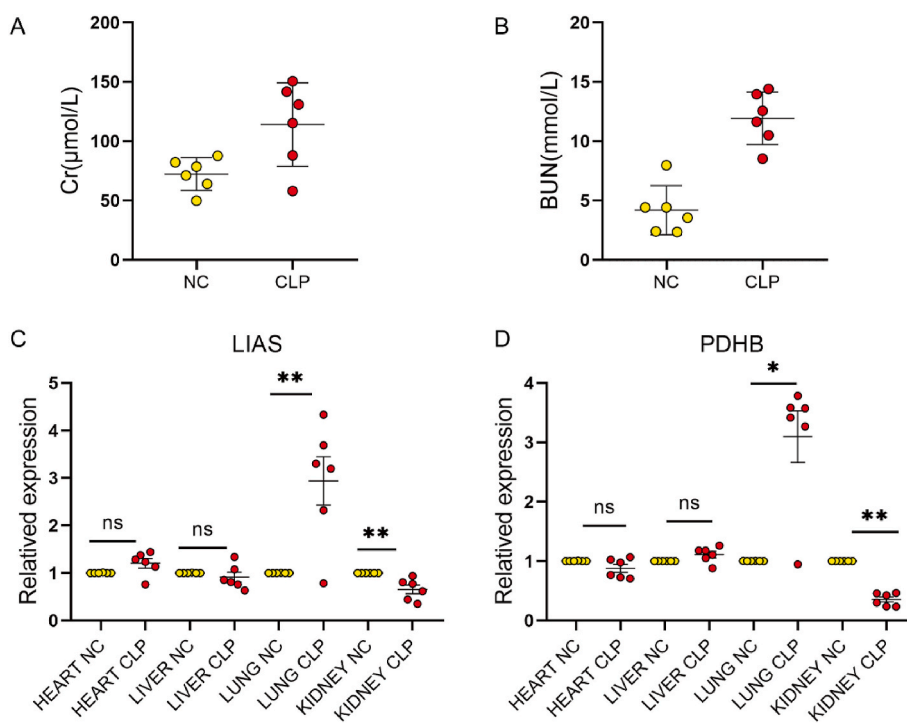


**Fig. 8.** (A) SCr levels in the controls and septic mice; (B) BUN levels in the controls and septic mice; (C) LIAS mRNA expression in heart, liver, lung and kidney of septic and normal mice; (D) PDHB mRNA expression in heart, liver, lung and kidney of septic and normal mice (n = 6, \*p < 0.05, \*\*p < 0.01).

response through adipokines. Our study indicates a correlation between PDHB downregulation and the onset of sepsis. Moreover, PDHB appears to be associated with T cell regulation in septic patients. This suggests that PDHB may contribute to metabolomic changes and oxidative stress resulting from mitochondrial dysfunction, while also influencing immune regulation in septic patients. These findings offer novel insights into utilizing PDHB as a potential diagnostic and therapeutic target for septic patients. However, further investigations are necessary to elucidate the specific molecular mechanisms involved.

The expression level of PDHB, a crucial enzyme in energy metabolism, may be influenced by physiological factors such as aging. With advancing age, there is a decrease in the energy demand, which can consequently lead to a reduction in the expression level of PDHB [40]. This decline in PDHB expression has the potential to disrupt the normal course of energy metabolism. Aging is often associated with the loss of muscle mass and strength, and studies have demonstrated lower PDHB gene expression in the muscles of aged mice compared to the younger ones. PDHB has been identified as a protective factor for muscle tissue by inhibiting the FoxP1-Arh2 axis, thus influencing skeletal muscle differentiation [41]. Consequently, understanding and modulating PDHB expression holds promise for addressing age-related muscle decline. In our study, we observed lower PDHB gene expression in aged patients with sepsis compared to younger patients. Aberrant PDHB expression has been associated with metabolic disorders such as lactic acidosis and metabolic acidosis [42], both of which disrupt cellular energy metabolism. Therefore, investigating age-related disparities in PDHB expression could offer insights into strategies for regulating it and maintaining normal energy metabolism.

The CRGs LIAS and PDHB demonstrate potential diagnostic value in the pathophysiology of sepsis, providing significant insights into the identification of new therapeutic targets. However, it is important to acknowledge certain limitations within our study. Firstly, our current understanding regarding the expression of CRGs has remained limited, and the precise molecular mechanisms of these genes in sepsis are not fully elucidated. Secondly, all the data presented in our study were sourced from publicly available datasets and have solely been validated in mouse models. Thus, further validation through clinical cohorts is imperative to comprehensively understand the role of LIAS and other CRGs in sepsis.

In our future research, we will address the limitations of our study by conducting experimental validation of cuproptosis-related genes. This will involve *in vitro* and *in vivo* studies to confirm their diagnostic potential and explore therapeutic implications in sepsis. To improve our understanding of sepsis pathogenesis, we plan to expand our investigation by including a larger and more diverse patient population. This broader sample will shed light on potential biomarkers and pathways involved in sepsis. Moreover, we will utilize alternative bioinformatic methods and databases to refine our analysis and identify additional biomarkers and pathways associated with sepsis. Collaborations with other research groups and an extensive literature review will augment our efforts.

Overall, our future research aims to enhance knowledge about the role of cuproptosis-related genes in sepsis pathogenesis and provide insights into diagnostic and therapeutic targets for this complex disease.



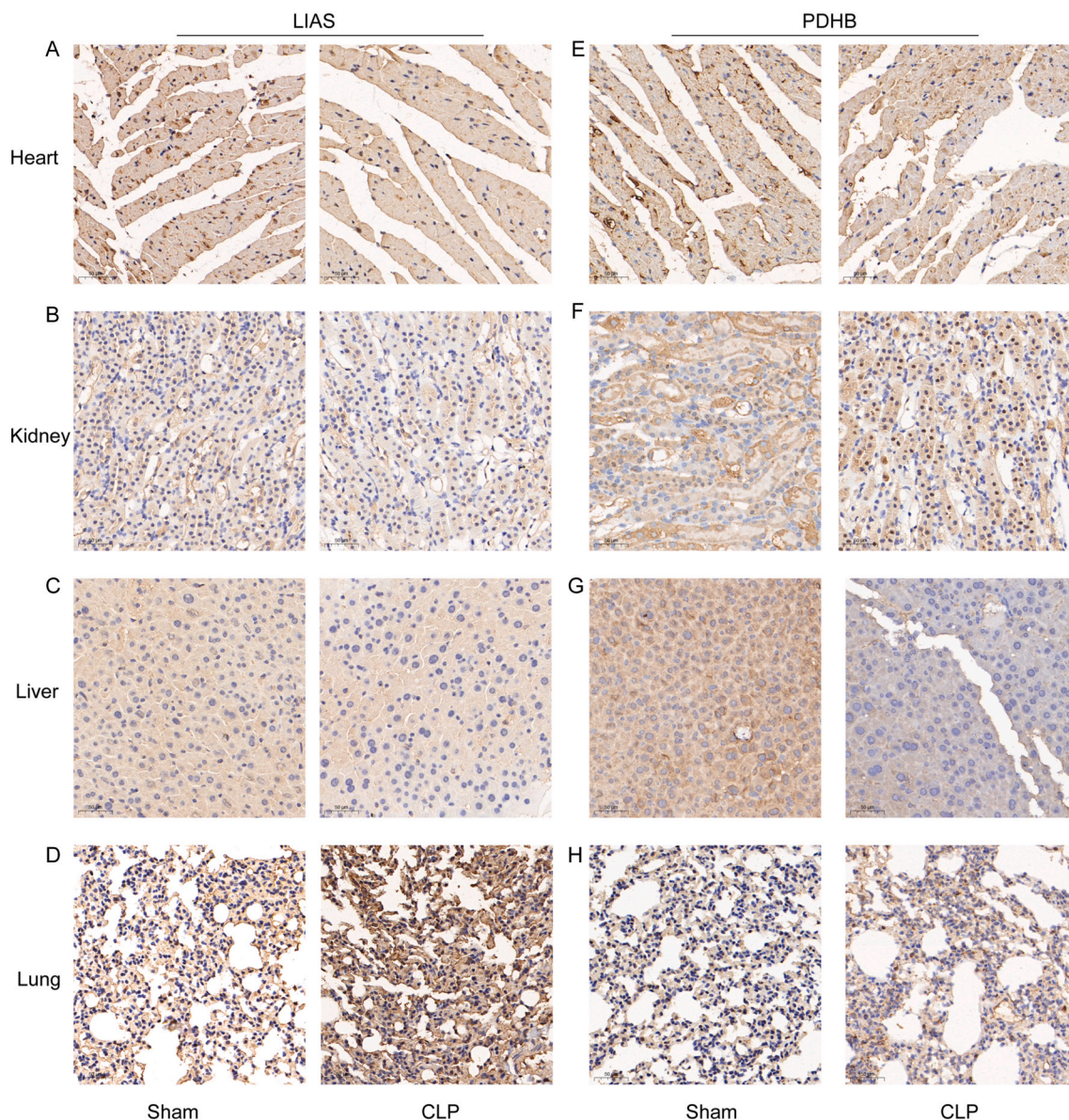


**Fig. 9.** (A) IHC staining for LIAS in heart; (B) IHC staining for LIAS in kidney; (C) IHC staining for LIAS in liver; (D) IHC staining for LIAS in lung; (E) IHC staining for PFHB in heart; (F) IHC staining for PDHB in kidney; (G) IHC staining for PDHB in liver; (H) IHC staining for PDHB in lung; (scale bars = 50 μm).

## 5. Conclusion

Our study has uncovered a potentially significant role of cuproptosis in the pathogenesis of sepsis. We have established a correlation between CRGs and sepsis, with a particular emphasis on LIAS and PDHB as promising biomarkers for sepsis diagnosis and prognosis. These findings offered novel insights into the underlying mechanisms connecting sepsis and cuproptosis, thereby providing valuable information on potential therapeutic targets and strategies. Further research is necessary to validate these biomarkers and investigate their clinical utility in enhancing sepsis diagnosis and improving patient outcomes.

## Data availability

Data associated with this study has been deposited at <https://www.ncbi.nlm.nih.gov/gds> under the accession number GSE65682 and GSE134347.

## Ethics statement

Animal experiments in this study were approved by the Animal Care and Use Committee of Wuhan University (IACUC: ZN2021182).

## Funding

This work was funded by the National Natural Science Foundation of China (grants 81772046 and 81971816 to Dr. Peng), and the Subject Cultivation Project of Zhongnan Hospital of Wuhan University (Zhiyong Peng, No. ZNXKPY2021001).

## CRedit authorship contribution statement

**Zhongyi Sun:** Conceptualization, Data curation, Formal analysis, Investigation, Methodology, Project administration, Software, Supervision, Validation, Visualization, Writing – original draft, Writing – review & editing. **Qiuyue Zhao:** Formal analysis, Writing – original draft, Writing – review & editing. **Jiahao Zhang:** Data curation, Formal analysis, Funding acquisition, Writing – original draft, Writing – review & editing. **Yanan Hu:** Data curation, Project administration, Resources. **Jiachen Qu:** Data curation, Project administration, Software. **Han Gao:** Formal analysis, Funding acquisition, Resources, Software, Validation, Visualization, Writing – original draft, Writing – review & editing. **Zhiyong Peng:** Conceptualization, Data curation, Formal analysis, Project administration, Supervision, Validation, Visualization, Writing – original draft, Writing – review & editing.

## Declaration of competing interest

The authors declare that they have no known competing financial interests or personal relationships that could have appeared to influence the work reported in this paper.

## Acknowledgements

The authors thankfully acquired the data provided by patients and researchers participating in GEO.

## Abbreviations

GEO	Gene expression omnibus
DEGs	Differentially expressed gene
CRG	Centre for genomic regulation
AUC	Area under the curve
ROC	Receiver operating characteristic curve
ssGSEA	Single-sample gene set enrichment analysis
GSEA	Gene set enrichment analysis
CLP	Cecal ligation and puncture
ELISA	Enzyme linked immunosorbent assay
qRT-PCR	Real-time quantitative PCR
IHC	Immunohistochemistry

## References

- [1] M. Cecconi, L. Evans, M. Levy, A. Rhodes, Sepsis and septic shock, *Lancet* 392 (2018) 75–87, [https://doi.org/10.1016/S0140-6736\(18\)30696-2](https://doi.org/10.1016/S0140-6736(18)30696-2).
- [2] N.A. Azadi, A. Ziapour, J.Y. Lebni, S.F. Irandoost, J. Abbas, F. Chaboksavar, The effect of education based on health belief model on promoting preventive behaviors of hypertensive disease in staff of the Iran University of Medical Sciences, *Arch Public Health* 79 (2021) 69, <https://doi.org/10.1186/s13690-021-00594-4>.
- [3] The state of health in Pakistan and its provinces and territories, 1990–2019: a systematic analysis for the Global Burden of Disease Study 2019, *Lancet Glob Health* 11 (2023) e229–e243, [https://doi.org/10.1016/S2214-109X\(22\)00497-1](https://doi.org/10.1016/S2214-109X(22)00497-1).
- [4] Z. Su, D. McDonnell, J. Wen, M. Kozak, J. Abbas, S. Şegalo, X. Li, J. Ahmad, A. Cheshmehzangi, Y. Cai, et al., Mental health consequences of COVID-19 media coverage: the need for effective crisis communication practices, *Global Health* 17 (2021) 4, <https://doi.org/10.1186/s12992-020-00654-4>.
- [5] C. Pierrakos, D. Velissaris, M. Bisdorff, J.C. Marshall, J.-L. Vincent, Biomarkers of sepsis: time for a reappraisal, *Crit. Care* 24 (2020) 287, <https://doi.org/10.1186/s13054-020-02993-5>.
- [6] H.C. Prescott, D.C. Angus, Enhancing recovery from sepsis: a review, *JAMA* 319 (2018) 62–75, <https://doi.org/10.1001/jama.2017.17687>.
- [7] C. Pierrakos, J.-L. Vincent, Sepsis biomarkers: a review, *Crit. Care* 14 (2010) R15, <https://doi.org/10.1186/cc8872>.
- [8] I. Bahar, G. Elay, G. Başkol, M. Sungur, H. Donmez-Altuntas, Increased DNA damage and increased apoptosis and necrosis in patients with severe sepsis and septic shock, *J. Crit. Care* 43 (2018) 271–275, <https://doi.org/10.1016/j.jcrc.2017.09.035>.
- [9] L. Liu, B. Sun, Neutrophil pyroptosis: new perspectives on sepsis, *Cell. Mol. Life Sci.* 76 (2019) 2031–2042, <https://doi.org/10.1007/s00018-019-03060-1>.
- [10] D. Glick, S. Barth, K.F. Macleod, Autophagy: cellular and molecular mechanisms, *J. Pathol.* 221 (2010) 3–12, <https://doi.org/10.1002/path.2697>.
- [11] C. Cao, M. Yu, Y. Chai, Pathological alteration and therapeutic implications of sepsis-induced immune cell apoptosis, *Cell Death Dis.* 10 (2019) 782, <https://doi.org/10.1038/s41419-019-2015-1>.

- [12] V. Oliveri, Selective targeting of cancer cells by copper ionophores: an overview, *Front. Mol. Biosci.* 9 (2022), 841814, <https://doi.org/10.3389/fmolb.2022.841814>.
- [13] Y. Wang, L. Zhang, F. Zhou, Cuproptosis: a new form of programmed cell death, *Cell. Mol. Immunol.* 19 (2022) 867–868, <https://doi.org/10.1038/s41423-022-00866-1>.
- [14] Z. Bian, R. Fan, L. Xie, A novel cuproptosis-related prognostic gene signature and validation of differential expression in clear cell renal cell carcinoma, *Genes* 13 (2022) 851, <https://doi.org/10.3390/genes13050851>.
- [15] G. Zhang, J. Sun, X. Zhang, A novel Cuproptosis-related LncRNA signature to predict prognosis in hepatocellular carcinoma, *Sci. Rep.* 12 (2022), 11325, <https://doi.org/10.1038/s41598-022-15251-1>.
- [16] X. Jiang, B.R. Stockwell, M. Conrad, Ferroptosis: mechanisms, biology and role in disease, *Nat. Rev. Mol. Cell Biol.* 22 (2021) 266–282, <https://doi.org/10.1038/s41580-020-00324-8>.
- [17] K. Hadian, B.R. Stockwell, The therapeutic potential of targeting regulated non-apoptotic cell death, *Nat. Rev. Drug Discov.* (2023), <https://doi.org/10.1038/s41573-023-00749-8>.
- [18] L. Xi, Z. Gy, R. G, N. C. Ferroptosis in sepsis: the mechanism, the role and the therapeutic potential, *Front. Immunol.* 13 (2022), 956361, <https://doi.org/10.3389/fimmu.2022.956361>.
- [19] A.C. Carr, G.M. Shaw, A.A. Fowler, R. Natarajan, Ascorbate-dependent vasopressor synthesis: a rationale for vitamin C administration in severe sepsis and septic shock? *Crit. Care* 19 (2015) 418, <https://doi.org/10.1186/s13054-015-1131-2>.
- [20] A. Roberts, D. Bar-Or, J.V. Winkler, L.T. Rael, Copper-induced oxidation of epinephrine: protective effect of D-DAHK, a synthetic analogue of the high affinity copper binding site of human albumin, *Biochem. Biophys. Res. Commun.* 304 (2003) 755–757, [https://doi.org/10.1016/s0006-291x\(03\)00667-3](https://doi.org/10.1016/s0006-291x(03)00667-3).
- [21] D. Bar-Or, L.T. Rael, J.V. Winkler, R.L. Yukl, G.W. Thomas, R.P. Shimonkevitz, Copper inhibits activated protein C: protective effect of human albumin and an analogue of its high-affinity copper-binding site, d-DAHK, *Biochem. Biophys. Res. Commun.* 290 (2002) 1388–1392, <https://doi.org/10.1006/bbrc.2002.6363>.
- [22] T. Barrett, S.E. Wilhite, P. Ledoux, C. Evangelista, I.F. Kim, M. Tomashevsky, K.A. Marshall, K.H. Phillippy, P.M. Sherman, M. Holko, et al., NCBI GEO: archive for functional genomics data sets—update, *Nucleic Acids Res.* 41 (2013) D991–D995, <https://doi.org/10.1093/nar/gks1193>.
- [23] P. Tsvetkov, S. Coy, B. Petrova, M. Dreishpoon, A. Verma, M. Abdusamad, J. Rossen, L. Joesch-Cohen, R. Humeidi, R.D. Spangler, et al., Copper induces cell death by targeting lipoylated TCA cycle proteins, *Science* 375 (2022) 1254–1261, <https://doi.org/10.1126/science.abb0529>.
- [24] D. Szklarczyk, A.L. Gable, D. Lyon, A. Junge, S. Wyder, J. Huerta-Cepas, M. Simonovic, N.T. Doncheva, J.H. Morris, P. Bork, et al., STRING v11: protein-protein association networks with increased coverage, supporting functional discovery in genome-wide experimental datasets, *Nucleic Acids Res.* 47 (2019) D607–D613, <https://doi.org/10.1093/nar/gky1131>.
- [25] C.-H. Chin, S.-H. Chen, H.-H. Wu, C.-W. Ho, M.-T. Ko, C.-Y. Lin, cytoHubba: identifying hub objects and sub-networks from complex interactome, *BMC Syst. Biol.* 8 (2014), <https://doi.org/10.1186/1752-0509-8-S4-S11>. Suppl 4:S11.
- [26] S.Y. Park, Nomogram: an analogue tool to deliver digital knowledge, *J. Thorac. Cardiovasc. Surg.* 155 (2018) 1793, <https://doi.org/10.1016/j.jtcvs.2017.12.107>.
- [27] S. Hänzelmann, R. Castelo, J. Guinney, GSEA: gene set variation analysis for microarray and RNA-seq data, *BMC Bioinf.* 14 (2013) 7, <https://doi.org/10.1186/1471-2105-14-7>.
- [28] A. Subramanian, P. Tamayo, V.K. Mootha, S. Mukherjee, B.L. Ebert, M.A. Gillette, A. Paulovich, S.L. Pomeroy, T.R. Golub, E.S. Lander, et al., Gene set enrichment analysis: a knowledge-based approach for interpreting genome-wide expression profiles, *Proc Natl Acad Sci U S A* 102 (2005) 15545–15550, <https://doi.org/10.1073/pnas.0506580102>.
- [29] A. Liberzon, C. Birger, H. Thorvaldsdóttir, M. Ghandi, J.P. Mesirov, P. Tamayo, The Molecular Signatures Database (MSigDB) hallmark gene set collection, *Cell Syst* 1 (2015) 417–425, <https://doi.org/10.1016/j.cels.2015.12.004>.
- [30] X. Cao, L. Zhu, X. Song, Z. Hu, J.E. Cronan, Protein moonlighting elucidates the essential human pathway catalyzing lipoic acid assembly on its cognate enzymes, *Proc Natl Acad Sci U S A* 115 (2018) E7063–E7072, <https://doi.org/10.1073/pnas.1805862115>.
- [31] J. Fan, C. Shan, H.-B. Kang, S. Elf, J. Xie, M. Tucker, T.-L. Gu, M. Aguiar, S. Lonning, H. Chen, et al., Tyr phosphorylation of PDP1 toggles recruitment between ACAT1 and SIRT3 to regulate the pyruvate dehydrogenase complex, *Mol Cell* 53 (2014) 534–548, <https://doi.org/10.1016/j.molcel.2013.12.026>.
- [32] I.F. Duarte, J. Caio, M.F. Moedas, L.A. Rodrigues, A.P. Leandro, I.A. Rivera, M.F.B. Silva, Dihydrolipoamide dehydrogenase, pyruvate oxidation, and acetylation-dependent mechanisms intersecting drug iatrogenesis, *Cell. Mol. Life Sci.* 78 (2021) 7451–7468, <https://doi.org/10.1007/s00018-021-03996-3>.
- [33] L. Packer, E.H. Witt, H.J. Tritschler, alpha-Lipoic acid as a biological antioxidant, *Free Radic. Biol. Med.* 19 (1995) 227–250, [https://doi.org/10.1016/0891-5849\(95\)00017-r](https://doi.org/10.1016/0891-5849(95)00017-r).
- [34] J. Vockley, Long-chain fatty acid oxidation disorders and current management strategies, *Am. J. Manag. Care* 26 (2020) S147–S154, <https://doi.org/10.37765/ajmc.2020.88480>.
- [35] D. Zhang, Z.-X. Liu, C.S. Choi, L. Tian, R. Kibbey, J. Dong, G.W. Cline, P.A. Wood, G.I. Shulman, Mitochondrial dysfunction due to long-chain Acyl-CoA dehydrogenase deficiency causes hepatic steatosis and hepatic insulin resistance, *Proc. Natl. Acad. Sci. U.S.A.* 104 (2007) 17075–17080, <https://doi.org/10.1073/pnas.0707060104>.
- [36] M.T. Lin, M.F. Beal, Mitochondrial dysfunction and oxidative stress in neurodegenerative diseases, *Nature* 443 (2006) 787–795, <https://doi.org/10.1038/nature05292>.
- [37] X. Yi, N. Maeda, Endogenous production of lipoic acid is essential for mouse development, *Mol Cell Biol* 25 (18) (2005 Sep) 8387–8392, <https://doi.org/10.1128/MCB.25.18.8387-8392.2005>.
- [38] J. Lee, D. Banerjee, Metabolomics and the microbiome as biomarkers in sepsis, *Crit. Care Clin.* 36 (2020) 105–113, <https://doi.org/10.1016/j.ccc.2019.08.008>.
- [39] X. Yi, L. Xu, S. Hiller, H.-S. Kim, V. Nickleit, L.R. James, N. Maeda, Reduced expression of lipoic acid synthase accelerates diabetic nephropathy, *J. Am. Soc. Nephrol.* 23 (2012) 103–111, <https://doi.org/10.1681/ASN.2011010003>.
- [40] E. Danileviciute, N. Zeng, C.M. Capelle, N. Paczia, M.A. Gillespie, H. Kurniawan, M. Benzarti, M.P. Merz, D. Coowar, S. Fritah, et al., PARK7/DJ-1 promotes pyruvate dehydrogenase activity and maintains Treg homeostasis during ageing, *Nat. Metab.* 4 (2022) 589–607, <https://doi.org/10.1038/s42255-022-00576-y>.
- [41] X. Jiang, S. Ji, F. Yuan, T. Li, S. Cui, W. Wang, X. Ye, R. Wang, Y. Chen, S. Zhu, Pyruvate dehydrogenase B regulates myogenic differentiation via the FoxP1-Arh2 axis, *J Cachexia Sarcopenia Muscle* 14 (2023) 606–621, <https://doi.org/10.1002/jcsm.13166>.
- [42] G.-F. Lu, F. Geng, L.-P. Deng, D.-C. Lin, Y.-Z. Huang, S.-M. Lai, Y.-C. Lin, L.-X. Gui, J.S.K. Sham, M.-J. Lin, Reduced CircSMOC1 level promotes metabolic reprogramming via PTBP1 (polypyrimidine tract-binding protein) and miR-329-3p in pulmonary arterial hypertension rats, *Hypertension* 79 (2022) 2465–2479, <https://doi.org/10.1161/HYPERTENSIONAHA.122.19183>.